

Experimental Study of Vibrational and Pure Rotational Coherent Anti-Stokes Raman Scattering (CARS) in Molecular Hydrogen

G. Marowsky, A. Gierulski, and B. Dick

Max-Planck-Institut für biophysikalische Chemie, Abteilung Laserphysik,
D-3400 Göttingen, Fed. Rep. Germany

U. Sowada and R. Vehrenkamp

Lambda Physik GmbH, P.O. Box 2663, D-3400 Göttingen, Fed. Rep. Germany

Received 23 May 1985/Accepted 24 August 1985

Abstract. Using a specially designed excimer-laser-pumped dye laser of adjustable bandwidth high-lying pure rotational transitions of both, ortho- and para-hydrogen have been identified by coherent anti-Stokes Raman scattering (CARS). As an interesting application H₂-based CARS-thermometry is discussed.

PACS: 42.65

Coherent anti-Stokes Raman spectroscopy (CARS) using rotational-vibrational transitions has proven to be a powerful tool in various areas of science and technology since its first demonstration by Maker and Terhune [1]. Use of pure rotational transitions, however, has been made so far only in a few applications dealing with concentration and temperature measurements of small molecules, such as H₂, N₂, O₂, N₂O, and CO [2–12]. It is the purpose of this paper to demonstrate that pure rotational CARS spectroscopy in the vibronic groundstate of molecular hydrogen is a very powerful tool for the detection of small concentrations of H₂, which can be utilized effectively for temperature measurements in various temperature ranges.

The principal difference in terms of energy levels used for rotational and vibrational CARS of hydrogen can be explained with reference to Fig. 1, showing the typical scattering processes taking place in a CARS-type experiment. The striking difference between vibrational and rotational CARS is the energy difference between the respective resonantly excited real levels,

such as ΔE_{vib} for the $v=0 \rightarrow v=1$ transition and ΔE_{rot} for the $J=1 \rightarrow J=3$ transition, which turned out to be the most intense rotational transition for H₂ trace analysis under room temperature conditions. The limits of detectability will be discussed in detail in Sect. 2.

1. Broadband Dye Laser

CARS spectra for concentration and temperature analysis are usually recorded by scanning the Stokes frequency ω_2 across a real vibrational or rotational state of the system under consideration (Fig. 2a) and observing the anti-Stokes emission of frequency $\omega_3 = \omega_A$ with a monochromator. An experimental alternative has been described by Roh et al. [13]. A broad-band dye laser of bandwidth $\Delta\omega$ is used in conjunction with a narrow-band pump laser to generate an entire anti-Stokes spectrum of transitions using a single laser pulse (Fig. 2b). Application of this technique resulted in the instantaneous generation of an entire Q-branch spectrum of molecular hydrogen.

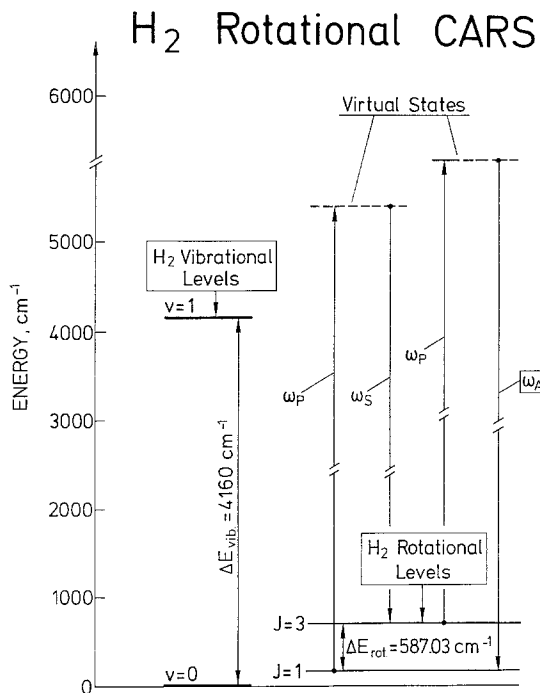
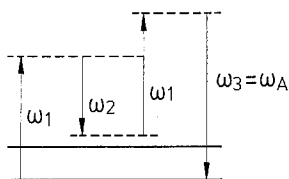


Fig. 1. Energy levels for rotational and, for comparison, vibrational transitions used for CARS experiments. ω_p and ω_s denote frequency of pump and Stokes laser, ω_A frequency of anti-Stokes emission. As example rotational levels of $J = 1 \rightarrow J = 3$ transitions are indicated

(a) Scanning-CARS



(b) Multiplex-CARS

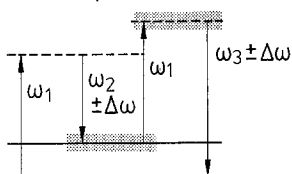


Fig. 2. (a) Energy levels for narrow-band scanning CARS technique, (b) schematic of multiplex CARS using a broad-band laser of halfwidth $\Delta\omega$ as Stokes laser

For optimized signal detection the bandwidth $\Delta\omega$ should just cover the frequency range of interest. The excimer-laser-pumped dye laser shown in Fig. 3 allows a convenient choice of the required bandwidth by adjusting the wavelength-selective grating to the ap-

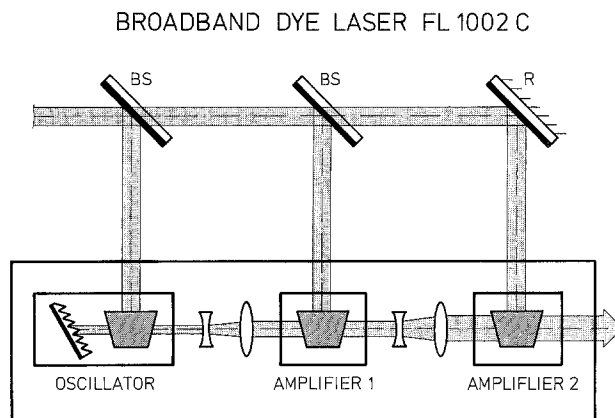


Fig. 3. Optical schematic of Lambda Physik broad-band dye laser type FL 1002 C

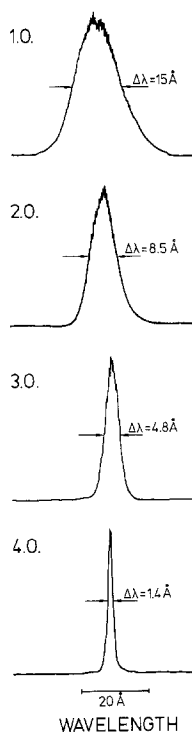


Fig. 4. Output spectra of broad-band dye laser obtained with four different settings of the oscillator diffraction grating (1.0 \cong first order etc.)

propriate order in retro-reflection. The oscillator of this laser consists only of a transversely pumped dye cell and a diffraction grating. Avoiding any normal glass surfaces, the radiation leaving the oscillator subsequently passes through a two-stage amplifier system. With an input energy of 100 mJ at the wavelength of XeCl (308 nm) the conversion efficiency in the red spectral range is typically 10%. Figure 4 shows a series of laser output spectra obtained by rotation of

the oscillator grating from first to fourth order, resulting in a variation of bandwidths from 15 to 1.4 Å. This laser has been used to examine one particular Q -branch transition of hydrogen at room temperature. Figure 5 shows for comparison an entire Q -branch spectrum (upper trace) of H_2 at a pressure of 100 Torr together with a Q_1 -spectrum at 2.5 Torr, taken with a Stokes-laser bandwidth reduced by a factor of 10. Taking into account the decrease in H_2 -density by a factor 40, the signal-intensity of Q_1 in the lower trace reflects an increase in spectral brightness by a factor by 10. The spectrum of Q_1 , shown for clarity on an expanded scale (500 vidicon channels $\cong 75 \text{ cm}^{-1}$), clearly indicates that with the narrowest available bandwidth (4.2 cm^{-1}) of the Stokes-laser no neighbouring Q -branch transitions are excited. In fact, according to [14] the spacing between Q_1 and Q_2 is 12 cm^{-1} . Rejection of the other transitions is an experimental indication that the Stokes-laser emission is sharply restricted to the bandwidth indicated. This avoids increase of the background level due to the short-wavelength tail of the dye fluorescence, which is a problem encountered in rotational CARS spectroscopy, when using a free-running dye laser with no intracavity wavelength-selective elements.

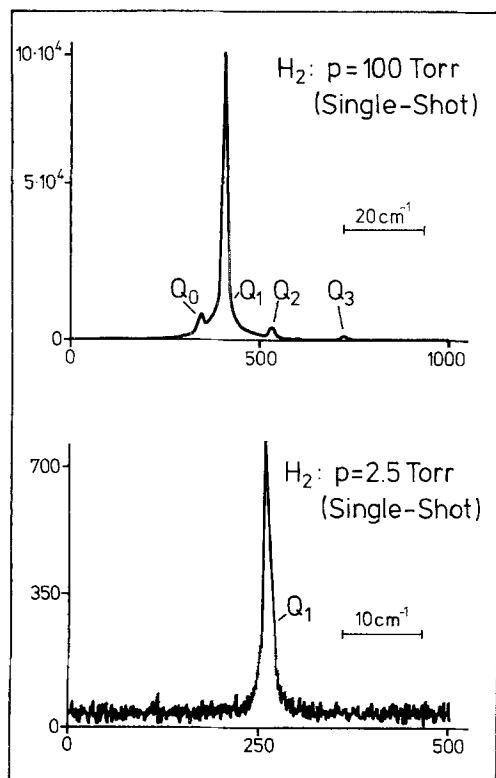


Fig. 5. Selection of Q_1 from H_2 Q -branch spectrum by appropriate reduction of broad-band dye-laser bandwidth

2. Experimental Set up

The experimental arrangement (Fig. 6) allowed the demonstration of visible CARS signals with the H_2 -cell operated at pressures in the atm-range and detection of low-density signals in the mTorr-range. Visual inspection was facilitated by a narrowband interference filter ($\Delta\lambda = 50 \text{ \AA}$) rejecting part of the intense pump- and Stokes-laser radiation and a dispersive grating for spatial separation of the collinear beams of wavelengths λ_p , λ_s , and λ_{AS} . The registration system for low H_2 -pressures consisted of a monochromator (Jobin Yvon 1 m double-monochromator) together with a triggered diode-array camera (OMA-III of PAR). Best results were obtained with a narrow-band dye laser (type FL 2002) and a broad-band dye laser (type FL 1002C). Both lasers are pumped with an excimer laser (type EMG 201 of 300 mJ typical pulse energy at 308 nm with XeCl). The dye lasers delivered 20 and 10 mJ, respectively, for pump and Stokes laser. The radiation of these lasers was combined by means of a dichroic beam splitter and focused with a lens of 30 cm focal length into the H_2 -cell. Figure 7 summarizes the relevant spectral data of pump, Stokes, and anti-Stokes wavelengths used in the course of these collinear, rotational CARS studies. For efficient rejection of the excitation radiation all experiments were centered around the transmission of a narrow-band interference filter that transmits in combination with the double-monochromator a spectral separation of the excitation wavelengths as low as

$$|\lambda_p - \lambda_s|_{\min} \geq 50 \text{ \AA}.$$

A separation of 50 Å or 150 cm^{-1} in this spectral range is sufficient for all rotational CARS studies with hydrogen. Table 1 lists the lowest rotational transitions in the vibronic groundstate of hydrogen [14]. The spectral separation of 50 Å is presumably too large for larger molecules such as CO, O_2 , and N_2 . Their rotational CARS analysis requires more-dimensional arrangements of the beam geometry as BOXCARS or even folded BOXCARS [15–17]. Due to the rather high signal levels no provisions were made to suppress the non-resonant background contribution by

Table 1. Transition energies of the lowest 6 rotational transitions $J \rightarrow J+2$ in hydrogen [14]

$J=0 \rightarrow J=2$	354 cm^{-1}
$J=1 \rightarrow J=3$	587 cm^{-1}
$J=2 \rightarrow J=4$	814 cm^{-1}
$J=3 \rightarrow J=5$	1035 cm^{-1}
$J=4 \rightarrow J=6$	1246 cm^{-1}
$J=5 \rightarrow J=7$	1448 cm^{-1}

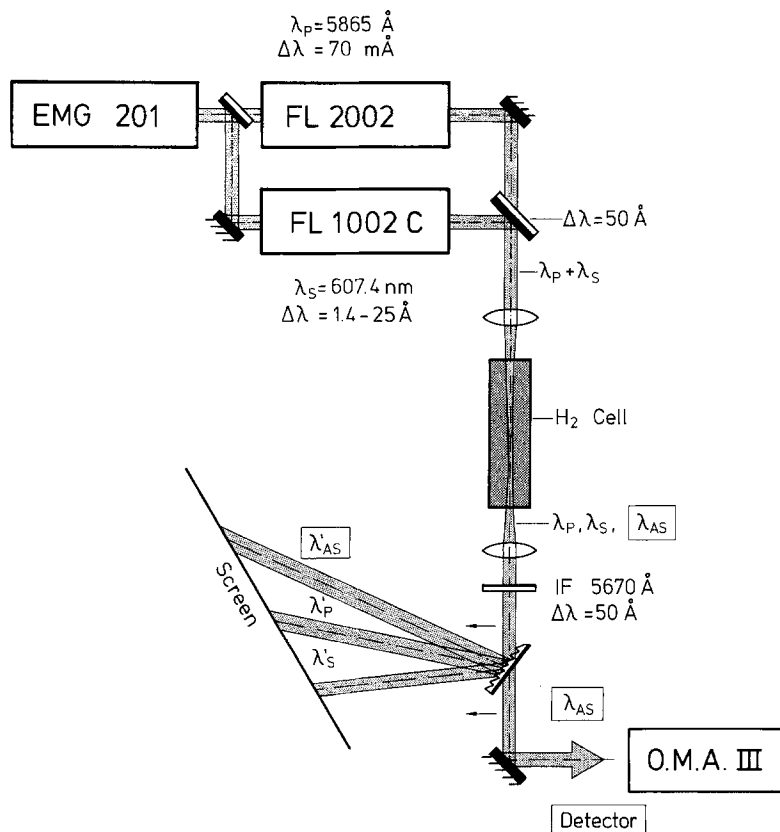


Fig. 6. Experimental setup for rotational H₂ CARS studies, allowing both, visual inspection of anti-Stokes radiation at a screen and sensitive detection with OMA-III diode-array camera after removal of diffraction grating

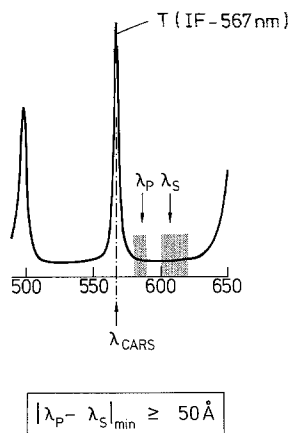


Fig. 7. Transmission characteristics of narrow-band interference filter centered at 5670 Å and spectral operation range of pump and Stokes laser

polarization-sensitive detection and appropriate polarization of the excitation beams [18–20]. The performance of the detection system in terms of linewidth is depicted in Fig. 8. The linewidth of the narrow-band pump laser (FL 2002) of 0.07 Å is beyond the resolving power of the monochromator-vidicon combination, yielding a technical width of 0.1 Å. When excited with a Stokes laser of 1.4 Å bandwidth, the width of the rotational CARS transitions is typically 0.2 Å and is also shown in Fig. 8.

3. Experimental Results

Relatively rare transitions of para-hydrogen and low H₂-concentrations were observed. In the literature so far only the $J=3 \rightarrow J=5$ and the $J=1 \rightarrow J=3$ transition [4,5] have been characterized by anti-Stokes Raman scattering.¹ So far nothing has been reported concerning the para-hydrogen species [21] with anti-parallel nuclear spin orientation. In addition, CARS signals are expected to be rather low due to the low concentration of para-hydrogen at room temperature. As an experimental result, all transitions indicated in Table 1 have been observed with CARS spectroscopy. With the excitation conditions, as described in Sect. 2, and a total H₂-pressure of 100 Torr the rotational transitions $J=4 \rightarrow J=6$ and $J=5 \rightarrow J=7$ could still be monitored (Fig. 9). Even higher transitions, such as $J=9 \rightarrow J=11$ which coincides with the fundamental, vibrational CARS mode of carbonmonoxide at 2131 cm⁻¹ are unavailable under room temperature conditions but have been recently observed in connection with combustion studies [5]. Table 2 summarizes limits of detection obtained for H₂ using the rotational

¹ Stimulated rotational Raman scattering in para-hydrogen is an efficient means of generating coherent radiation in the 13–18 μm region [25]

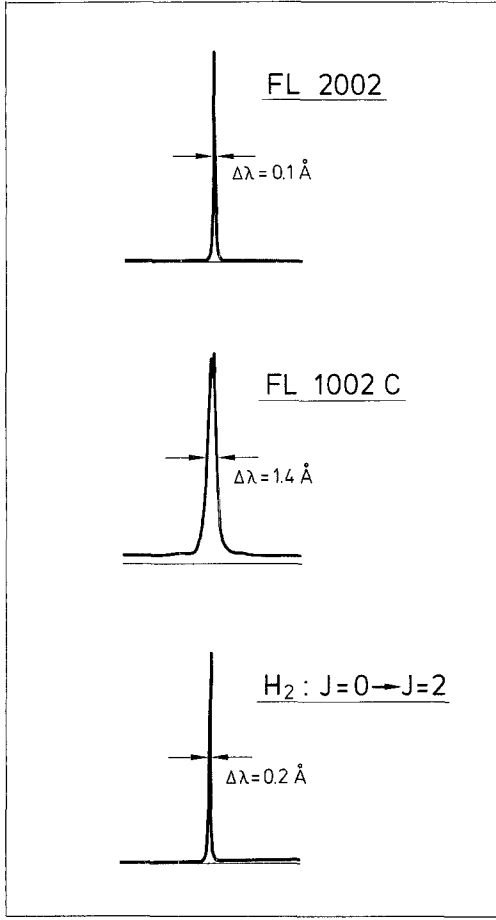


Fig. 8. Output spectra of the FL2002 and FL1002C lasers together with $J=0 \rightarrow J=2$ rotational CARS line

$J=1 \rightarrow J=3$ transition and the Q_1 -band of the vibrational branch for comparison.

The first row refers to single-shot spectra with subtraction of the background due to electrical noise of the diode-array camera and due to scattering light in the detection system. Long time averaging refers to collection of up to 10^4 laser shots.

The apparent difference in sensitivity between rotational and vibrational transitions (Table 2) can be explained in terms of the resonant enhancement of the nonlinear susceptibility $\chi^{(3)}$. The generated power of the CARS signal is proportional to the square of the pump laser intensity I_1 , the Stokes-laser intensity I_2 , and the square modulus of the susceptibility $\chi^{(3)}$

$$P^{\text{CARS}} \sim I_1^2 \cdot I_2 \cdot |\chi^{(3)}|^2. \quad (1)$$

Close to resonance the susceptibility is given by

$$\chi^{(3)} = \frac{N}{h} \sum_{a,b} (\varrho_a - \varrho_b) \frac{c^4}{\omega_1 \omega_2^3} \left(\frac{d\sigma}{d\Omega} \right)_{ab} \frac{1}{\omega_{ba} - \omega_1 + \omega_2 + i\Gamma_{ab}}. \quad (2)$$

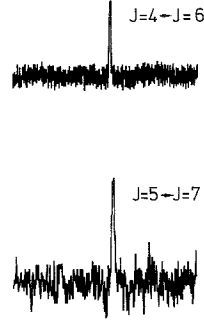


Fig. 9. Rotational CARS spectra of vibrational ground state

In this expression N is the number density, $d\sigma/d\Omega$ the Raman cross section for the transition $|a\rangle \rightarrow |b\rangle$, ϱ_a the population of level $|a\rangle$, and Γ_{ab} the Raman linewidth. For low concentrations at room temperature the linewidth is dominated by the Doppler width Γ_D which is proportional to the Stokes shift. Thus on resonance,

$$|\chi^{(3)}| \sim 1/\Gamma_D \sim \frac{1}{\omega_1 - \omega_2}. \quad (3)$$

Therefore, rotational CARS resonances ($\omega_1 - \omega_2 = 587 \text{ cm}^{-1}$) should be enhanced by almost two orders of magnitude with respect to vibrational CARS resonances ($\omega_1 - \omega_2 = 4160 \text{ cm}^{-1}$) due to the linewidth. In addition, pure rotational Raman cross sections are usually much larger than those for vibrational Q -branch transitions. On the other hand, the population difference factor might be smaller for rotational transitions. For a purely rotational transition $J \rightarrow J+2$, (2) must be summed over all degenerate levels of the initial and final state. For thermal equilibrium the J -dependent part of the susceptibility is

$$\chi^{(3)}(J \rightarrow J+2) \sim \frac{N}{Q(T)} \cdot \frac{(J+1)(J+2)}{(2J+3)} \cdot [X(J, T) - X(J+2, T)], \quad (4)$$

$$X(J, T) = g_J \cdot \exp[-E(J)/kT],$$

$$Q(T) = \sum_{J,v} g_J (2J+1) \exp[-E(J, v)/kT],$$

$$E(J, v) = E_v^0 + B_v J(J+1) + D_v J^2(J+1)^2 + H_v J^3(J+1)^3.$$

Table 2. Detection limits for H_2 with rotational and vibrational CARS with the apparatus used

	Rot. CARS	Vib. CARS
Single shot	10 mTorr	100 mTorr
Long-time averaging	1 mTorr	10 mTorr

Here B_v , D_v , and H_v are the rotational constants in the vibrational state v with vibrational energy E_v^0 , and g_J is the nuclear spin weight:

$$g_J = \begin{cases} 3 & \text{for } J \text{ odd (ortho-H}_2\text{)} \\ 1 & \text{for } J \text{ even (para-H}_2\text{)} \end{cases}$$

The conversion between ortho- and para-hydrogen is spin-forbidden and slow in the absence of a catalyst. Therefore, after a change of temperature, the system behaves as a mixture of two species with their own total populations and partition functions $Q(T)$. In this case N in (4) must be replaced by N_o or N_p , and the sum in $Q(T)$ runs over odd J or even J for ortho- or para-hydrogen, respectively.

In the intensity ratio of two transitions both in ortho- or both in para-H₂ the partition functions and population factors cancel and the temperature can be determined.

The intensity ratio of a transition in ortho-H₂ and in para-H₂ contains the population ratio N_o/N_p as an additional variable which can be determined when the temperature is known. This could be used to check whether equilibrium between both modifications has been achieved at the new temperature, or to follow the kinetics of the ortho \leftrightarrow para conversion. A thermometer based upon pure rotational transitions is represented in Fig. 10. The intensities of the lowest 6 transitions are shown as a function of temperature for a H₂-system in thermal equilibrium. The whole temperature range depicted in Fig. 10 is experimentally accessible from the standpoint of detection sensitivity. Each pair of transitions constitutes a potential CARS

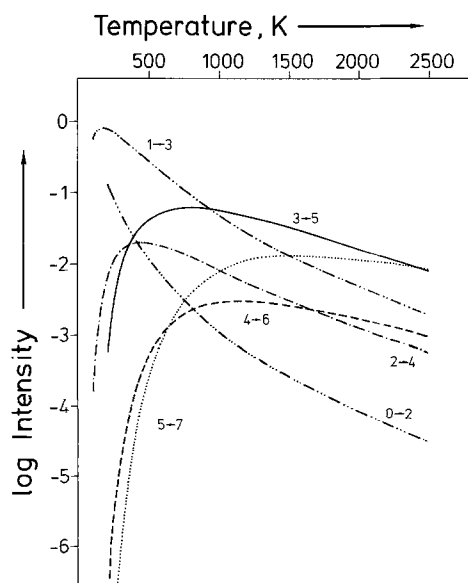


Fig. 10. Intensities of the lowest 6 rotational CARS transitions as a function of temperature. A Boltzmann distribution of populations was assumed. Rotational constants were taken from [14]

thermometer. The best choice are transitions with strongly different slopes in Fig. 10. The pair $0 \rightarrow 2/2 \rightarrow 4$ could be used from room temperature up to ca. 1000 K, the pair $1 \rightarrow 3/3 \rightarrow 5$ in the range from 500 to 1500 K, and the pairs $3 \rightarrow 5/5 \rightarrow 7$ and $2 \rightarrow 4/4 \rightarrow 6$ in the whole range up to 2500 K. All these thermometers do not depend on the relative population of the ortho- and para-H₂ level systems. However, they have the disadvantage that the transitions involved are spectrally far apart. That makes it difficult to measure the intensities under identical conditions, since interference filters, adjustment and even the laser dye would have to be changed.

An experimental alternative would be to monitor simultaneously a $\Delta J = 2$ transition in the $v = 0$ and $v = 1$ band. The spectral separation is as follows [14]:

$$J = 0 \rightarrow J = 2: 17.7 \text{ cm}^{-1},$$

$$J = 1 \rightarrow J = 3: 29.4 \text{ cm}^{-1},$$

$$J = 2 \rightarrow J = 4: 40.9 \text{ cm}^{-1}.$$

Thus each pair is easily accessible by the multiplex method, provided the population is high enough in the first vibronically excited state.

4. Conclusions

The first 6 low-lying rotational transitions of ortho- and para-hydrogen have been investigated by multiplex coherent anti-Stokes Raman spectroscopy (CARS) using two excimer laser pumped dye lasers. The transition $J = 1 \rightarrow J = 3$ allows H₂ concentration measurements down to 1 mTorr, which represents an one order of magnitude improvement compared to vibrational CARS using the Q_1 -mode of the Q -branch. A CARS thermometer based upon intensity ratios of individual rotational transitions is proposed.

Acknowledgements. We thank Lambda Physik and Princeton Applied Research for the loan of equipment.

References

1. P.D. Maker, R.W. Terhune: *Phys. Rev.* **137**, A801 (1965)
2. J.J. Barrett: *Appl. Phys. Lett.* **29**, 722 (1976)
3. I.R. Beattie, T.R. Gilson, D.A. Greenhalgh: *Nature* **276**, 378 (1978)
4. L.P. Goss, J.W. Fleming, A.B. Harvey: *Opt. Lett.* **5**, 345 (1980)
5. D. Klick, K.A. Marko, L. Rimai: *Appl. Opt.* **20**, 1178 (1981)
6. L.E. Harris: *Chem. Phys. Lett.* **93**, 335 (1982)
7. L.E. Harris: *Combustion Flame* **53**, 103 (1983)
8. D.V. Murphy, R.K. Chang: *Opt. Lett.* **6**, 233 (1981)
9. K. Aron, L.E. Harris, J. Fendell: *Appl. Opt.* **22**, 3604 (1983)

10. K. Aron, L.E. Harris, J. Fendell: Techn. Rep. ARLCD-TR-83033; U.S. Army Armament Research and Development Center, Dover, NJ, USA (August 1983)
11. J. Fendell, L.E. Harris, K. Aron: Techn. Rep. ARLCD-TR-83048; U.S. Army Armament Research and Development Center, Dover, NJ, USA (December 1983)
12. Jia-biao Zheng, J.B. Snow, D.V. Murphy, A. Leipertz, R.K. Chang: Opt. Lett. **9**, 341 (1984)
13. W.B. Roh, P.W. Schreiber, J.P.E. Taran: Appl. Phys. Lett. **29**, 174 (1976)
14. U. Fink, T.A. Wiggins, D.H. Rank: J. Mol. Spectrosc. **18**, 384 (1965)
15. A.C. Eckbreth: Appl. Phys. Lett. **32**, 421 (1978)
16. J.A. Shirley, R.J. Hall, A.C. Eckbreth: Opt. Lett. **5**, 380 (1980)
17. J.B. Snow, Jia-biao Zheng, R.K. Chang: Opt. Lett. **8**, 599 (1983)
18. J.J. Song, G.L. Eesley, M.D. Levenson: Appl. Phys. Lett. **29**, 567 (1976)
19. L.A. Rahn, L.J. Zych, P.L. Mattern: Opt. Commun. **30**, 249 (1979)
20. T. Dreier, U. Wellhausen, J. Wolfrum, G. Marowsky: Appl. Phys. B **29**, 31 (1982)
21. G. Herzberg: *Molecular Spectra and Molecular Structure, I. Spectra of Diatomic Molecules* (Van Nostrand Reinhold, New York 1950)
22. W.M. Tolles, J.W. Nibler, J.R. McDonald, A.B. Harvey: Appl. Spectrosc. **31**, 253 (1977)
23. J.W. Nibler, J.R. McDonald, A.B. Harvey: Opt. Commun. **18**, 371 (1976)
24. W. Kreutner, W. Stricker, Th. Just: Ber. Bunsenges. Phys. Chem. **87**, 1045 (1983)
25. H. Tashiro et al.: Opt. Lett. **10**, 80 (1985)